ECMWF COPERNICUS REPORT

Copernicus Climate Change Service

Product Quality Assessment Report (PQAR) – ANNEX E for IASI CO_2 and CH_4 (v9.1) and AIRS CO_2 mid-tropospheric products

C3S_312b_Lot2_DLR – Atmosphere

Issued by: C. Crevoisier, LMD/CNRS, France

Date: 18/02/2021

Ref: C3S_D312b_Lot2.2.2.3-v3.0_PQAR-GHG_ANNEX-E_v5.0

Official reference number service contract: 2016/C3S_312b_Lot2_DLR/SC1

Contributors

INSTITUTE OF ENVIRONMENTAL PHYSICS (IUP), UNIVERSITY OF BREMEN, BREMEN, GERMANY
(IUP)
M. Buchwitz

CENTRE NATIONAL DE LA RECHERCHE SCIENTIFIQUE (CNRS), LABORATOIRE DE METEOROLOGIE DYNAMIQUE (LMD), PALAISEAU, FRANCE
(LMD/CNRS)
C. Crevoisier
R. Armante

Table of Contents

History of modifications

Version	Date	Description of modification	Chapters / Sections
1.1	20-October-2017	New document for data set CDR1 (until 2016)	All
2.0	4-October-2018	Update for CDR2 (until 2017)	All
3.0	12-August-2019	Update for CDR3 (until 2018) and additional information of Metop-C	All, esp. Sects. 1.1 and 2.1
3.1	03-November-2019	Update after review by Assimila: Correction of typos and broken links. Some references added.	All
4.0 beta	18-August-2020	Update for CDR4 (until 2019) with new version of each IASI product	All
4.0	17-September-2020	Correction of issues with numbering of tables and figures based on review by Assimila	All
5.0	18-February-2021	Update for CDR5 (until 2020)	All

Related documents

Reference ID	Document
D1	Main PQAR: Buchwitz, M., et al., Product Quality Assessment Report (PQAR) – Main document for Greenhouse Gas (GHG: CO_2 & CH_4) data set CDR 5 (01.2003-06.2020), project C3S_312b_Lot2_DLR – Atmosphere, v5.0, 2021. *(this document is an ANNEX to the Main PQAR)*
D2	Crevoisier, C., et al., Algorithm Theoretical Basis Document (ATBD) – ANNEX E for IASI CO_2 and CH_4 and AIRS CO_2 mid-tropospheric products, project C3S_312b_Lot2_DLR – Atmosphere, v5.0, 2021.

Acronyms

Acronym	Definition
AIRS	Atmospheric Infrared Sounder
AMSU	Advanced Microwave Sounding Unit
ATBD	Algorithm Theoretical Basis Document
BESD	Bremen optimal EStimation DOAS
CAR	Climate Assessment Report
C3S	Copernicus Climate Change Service
CCDAS	Carbon Cycle Data Assimilation System
CCI	Climate Change Initiative
CDR	Climate Data Record
CDS	(Copernicus) Climate Data Store
CMUG	Climate Modelling User Group (of ESA's CCI)
CoMet	Carbon Dioxide and Methane Mission
CONTRAIL	Comprehensive Observation Network for Trace gases by Airlines
CRG	Climate Research Group
D/B	Data base
DOAS	Differential Optical Absorption Spectroscopy
EC	European Commission
ECMWF	European Centre for Medium Range Weather Forecasting
ECV	Essential Climate Variable
EMMA	Ensemble Median Algorithm
ENVISAT	Environmental Satellite (of ESA)
EO	Earth Observation
ESA	European Space Agency
EU	European Union
EUMETSAT	European Organisation for the Exploitation of Meteorological Satellites
FCDR	Fundamental Climate Data Record
FoM	Figure of Merit
FP	Full Physics retrieval method
FTIR	Fourier Transform InfraRed
FTS	Fourier Transform Spectrometer
GCOS	Global Climate Observing System
GEO	Group on Earth Observation
GEOSS	Global Earth Observation System of Systems
GHG	GreenHouse Gas
GOME	Global Ozone Monitoring Experiment
GMES	Global Monitoring for Environment and Security

HIPPO	HIAPER Pole-to-Pole Observations
GOSAT	Greenhouse Gases Observing Satellite
IAGOS	In-service Aircraft for a Global Observing System
IASI	Infrared Atmospheric Sounding Interferometer
ICOS	Integrated Carbon Observation System
IMAP-DOAS (or IMAP)	Iterative Maximum A posteriori DOAS
IPCC	International Panel in Climate Change
IUP	Institute of Environmental Physics (IUP) of the University of Bremen, Germany
JAXA	Japan Aerospace Exploration Agency
JCGM	Joint Committee for Guides in Metrology
L1	Level 1
L2	Level 2
L3	Level 3
L4	Level 4
LMD	Laboratoire de Météorologie Dynamique
MACC	Monitoring Atmospheric Composition and Climate, EU GMES project
NA	Not applicable
NASA	National Aeronautics and Space Administration
NetCDF	Network Common Data Format
NDACC	Network for the Detection of Atmospheric Composition Change
NIES	National Institute for Environmental Studies
NIR	Near Infra Red
NLIS	LMD/CNRS *neuronal* network mid/upper tropospheric CO2 and CH4 retrieval algorithm
NOAA	National Oceanic and Atmospheric Administration
Obs4MIPs	Observations for Climate Model Intercomparisons
OCO	Orbiting Carbon Observatory
OE	Optimal Estimation
PBL	Planetary Boundary Layer
ppb	Parts per billion
ppm	Parts per million
PR	(light path) PRoxy retrieval method
PVIR	Product Validation and Intercomparison Report
QA	Quality Assurance
QC	Quality Control
REQ	Requirement
RMS	Root-Mean-Square
RTM	Radiative transfer model
SCIAMACHY	SCanning Imaging Absorption spectroMeter for Atmospheric ChartographY
SCIATRAN	SCIAMACHY radiative transfer model

SRON	SRON Netherlands Institute for Space Research
SWIR	Short Wava Infra Red
TANSO	Thermal And Near infrared Sensor for carbon Observation
TANSO-FTS	Fourier Transform Spectrometer on GOSAT
TBC	To be confirmed
TBD	To be defined / to be determined
TCCON	Total Carbon Column Observing Network
TIR	Thermal Infra Red
TR	Target Requirements
TRD	Target Requirements Document
WFM-DOAS (or WFMD)	Weighting Function Modified DOAS
UoL	University of Leicester, United Kingdom
URD	User Requirements Document
WMO	World Meteorological Organization
Y2Y	Year-to-year (bias variability)

General definitions

Table 1 lists some general definitions relevant for this document.

Table 1: General definitions.

Item	Definition
XCO_2	Column-averaged dry-air mixing ratios (mole fractions) of CO_2
XCH_4	Column-averaged dry-air mixing ratios (mole fractions) of CH_4
L1	Level 1 satellite data product: geolocated radiance (spectra)
L2	Level 2 satellite-derived data product: Here: CO_2 and CH_4 information for each ground-pixel
L3	Level 3 satellite-derived data product: Here: Gridded CO_2 and CH_4 information, e.g., 5 deg times 5 deg, monthly
L4	Level 4 satellite-derived data product: Here: Surface fluxes (emission and/or uptake) of CO_2 and CH_4

Scope of document

This document is a Product Quality Assessment Report (PQAR) for the Copernicus Climate Change Service (C3S, https://climate.copernicus.eu/) greenhouse gas (GHG) component as covered by project C3S_312b_Lot2.

Within this project satellite-derived atmospheric carbon dioxide (CO_2) and methane (CH_4) Essential Climate Variable (ECV) data products will be generated and delivered to ECMWF for inclusion into the Copernicus Climate Data Store (CDS) from which users can access these data products and the corresponding documentation.

The satellite-derived GHG data products are:

- Column-average dry-air mixing ratios (mole fractions) of CO_2 and CH_4, denoted XCO_2 (in parts per million, ppm) and XCH_4 (in parts per billion, ppb), respectively.
- Mid/upper tropospheric mixing ratios of CO_2 (in ppm) and CH_4 (in ppb).

This document describes the validation / quality assessment of the C3S products CO2_IASA_NLIS (v9.1), CH4_IASA_NLIS (v9.1), CO2_IASB_NLIS (v9.1), CH4_IASB_NLIS (v9.1), CO2_AIRS_NLIS (v3.0).

These products are mid-tropospheric CO_2 and CH_4 Level 2 products as retrieved from the IASI sensors on Metop-A and Metop-B and mid-tropospheric CO_2 from AIRS using algorithms developed at CNRS-LMD, France.

Executive summary

This document describes the performance for the Level 2 CO_2 and CH_4 data products retrieved from IASI observations at CNRS-LMD and delivered to the Copernicus Climate Change Service (C3S). These products are mid-tropospheric-averaged dry-air mixing ratios (mole fractions) of CH_4 and CO_2, retrieved at 9:30 am/pm (local time) from observations made by the IASI and AMSU instruments onboard the European Metop-A (since July 2006) and Metop-B (since February 2013) platforms, and mid-tropospheric-averaged dry-air mixing ratios (mole fractions) of CO_2, retrieved at 13:30 am/pm (local time) from observations made by the AIRS and AMSU instruments onboard NASA Aqua platform.

IASI and AIRS observations were spatially and temporally collocated with observations made from aircraft measurements from the CONTRAIL (*Machida et al., 2007, 2008; Matsueda et al., 2008; Sawa et al., 2015*) and HIPPO (*Wofsy et al. 2012*) programs, as well as with observations made from balloons using AirCores (*Membrive et al., 2017*). When enough in-situ data were available, a number of statistics, including accuracy and stability, have been computed from the difference between in-situ measurements and retrievals from space observation. Overall, the CNRS-LMD products are found to be highly stable and meet the Target Requirement (TR) requirements for accuracy and stability. It has to be noted that, due to too sparse a validation data for CH_4, the TR for stability could not be computed. This calls for continuous effort in performing and developing continuous airborne observations of greenhouse gases.

1. Product validation methodology

1.1 CH_4 and CO_2 mid-tropospheric column averaged mole fractions

The validation is performed for five Level 2 products:

- CO2_IASA_NLIS: mid-tropospheric column averaged mole fractions of CO_2 retrieved from IASI onboard Metop-A.
- CO2_IASB_NLIS: mid-tropospheric column averaged mole fractions of CO_2 retrieved from IASI onboard Metop-B.
- CH4_IASA_NLIS: mid-tropospheric column averaged mole fractions of CH_4 retrieved from IASI onboard Metop-A.
- CH4_IASB_NLIS: mid-tropospheric column averaged mole fractions of CH_4 retrieved from IASI onboard Metop-B.
- CO2_AIRS_NLIS: mid-tropospheric column averaged mole fractions of CO_2 retrieved from AIRS onboard Aqua.

The four first products have been retrieved from simultaneous observations of the IASI and AMSU instruments flying together onboard the Metop satellites using a non-linear inference scheme using Multi-Layer Perceptrons with 2 hidden layers. IASI hyperspectral observations in the thermal infrared at 7.7 µm (resp. 15 µm), which are sensitive to both temperature and gas concentrations of CH_4 (resp. CO_2) are used in conjunction with microwave observations from the AMSU instruments, only sensitive to temperature, to decorrelate both signals (*Crevoisier et al., 2009a, 2009b, 2013*). The fifth product has been similarly obtained with AIRS and AMSU observations.

Potential radiative systematic biases existing between simulations used in the inference scheme and observations are computed for each channel by averaging, over the instruments full years of operation, the differences between simulations and collocated (in time and space) satellite observations. The simulations are performed using the 4A/OP-2009 forward model (*Scott and Chédin, 1981*; https://4aop.noveltis.com/), which is based on the updated 2011 version of the GEISA spectroscopic database (available at https://geisa.aeris-data.fr/) (*Jacquinet-Husson et al., 2011*), and radiosonde measurements from the Analyzed Radio Soundings Archive database (available at http://ara.lmd.polytechnique.fr). IASI calibrated radiance spectra (level1c) are received through the EUMETCast near real time data distribution service via the French AERIS center (https://www.aeris-data.fr/).

The retrieved CO_2 and CH_4 integrated columns are weighted to the tropical mid-troposphere with peak sensitivity at about 230 hPa (~11 km), half the peak sensitivity at 100 and 500 hPa (~6 and 16 km), and no sensitivity to the surface. Retrievals are performed over land and sea, by night and day (9:30 am/pm local time) for clear-sky only (no clouds, no aerosols). The CO_2 retrievals are limited to the tropical region (30N:30S) because of the greater stability of the temperature atmospheric profile, which helps decorrelating temperature from gas in the observed radiances, yielding a much better precision compared to the extratropics.

In order to cope with failure of various AMSU channels on each Metop satellites, version 9.1 of the retrieval has been designed to process the entire time series of Metop-A and Metop-B data with the same retrieval code that excludes all failed AMSU channels. This yields a homogeneous data set of mid-tropospheric CH_4 and CO_2 from both instruments over the entire time period since the first launch of IASI onboard Metop-A.

1.2 Validation data and method

Validation against high precision / low systematic errors reference observations is required for the mid/upper troposphere CO_2 and CH_4 data products. Unfortunately, measurements of both gases in the free troposphere and stratosphere are every sparse. Validation thus mostly relies on existing aircraft and airborne measurements.

A promising way consists in using 0-30 km profiles measured by balloon-borne AirCores (*Karion et al., 2010; Membrive et al., 2017*) to which averaging kernels can be applied to derive columns that can then be compared to those derived from space. So far, only a few profiles have been acquired, all in the northern hemisphere. In this validation exercise, use is made of CH_4 profiles measured by the French AirCore program (https://aircore.aeris-data.fr) at various stations located in France (Aire-sur-l'Adour, Trainou, Reims) as well as in Canada (Timmins, Ontario) and Sweden (Kiruna). Additional profiles comes from Sodankylä (Finland). Spanning 2014-2019, they are used to validate both Metop-A and Metop-B retrievals (CH4_IASA_NLIS and CH4_IASB_NLIS).

2. Validation Results

2.1 Products CO2_IASA_NLIS and CO2_IASB_NLIS

2.1.1 Validation

2.1.1.1 Validation with aircraft measurements

Figure 1 shows comparison of IASI CO_2 mid-tropospheric columns with commercial aircraft measurements made as part of the CONTRAIL project (*Matsueda et al. 2008, Machida et al., 2008, Sawa et al., 2015*) as monthly means in 12 latitudinal bands of 5° each. Figure 2 shows the scatter plot of IASI CO_2 vs. CONTRAIL CO_2 for the whole period. The R correlation coefficient is 0.98 for IASI-A (v9.1) and 0.92 for IASI-B (v9.1), the bias and the standard deviation of the difference between both being 0.96 ± 1.20 ppm. The bias for v9.1 is larger than for previous version (the difference was 0.57 ± 0.99 ppmv for CRDP3). This might come from the change in the retrieval code that has led to a change in the vertical sensitivity to CO_2 variations as explained in ATBD_ANNEX-E v4.0. With a higher sensitivity to CO_2 at lower altitudes than previous versions, the difference between the partial column retrieved from IASI and the in-situ concentration measured at 11-12 km by CONTRAIl is expected to be higher.

To compute the various parameters summarized in the following tables, the time series in each latitudinal band displayed in Figure 1 have been used separately.

Table 2 shows the mean CONTRAIL-IASI-A CO_2 difference together with the associated standard deviation recorded in each latitudinal band. The mean CONTRAIL-IASI-A bias over all latitudinal band is 0.96 ppm.

Table 2: Mean and standard deviation of CO_2 (ppm): difference between CONTRAIL and IASI (v9.1) over 12 latitudinal bands of 5° each. Statistics over July 2007-December 2019.

Latitudinal band	30S: 25S	25S: 20S	20S: 15S	15S: 10S	10S: 5S	5S :EQ	EQ: 5N	5N: 10N	10N: 15N	15N: 20N	20N: 25N	25N: 30N
IASI-CONTRAIL	2.80 +/- 1.52	1.88 +/- 1.45	0.94 +/- 1.31	0.27 +/- 1.17	-0.11 +/- 1.15	0.01 +/- 1.18	0.27 +/- 1.29	0.24 +/- 1.17	0.38 +/- 0.99	0.99 +/- 1.00	1.58 +/- 1.04	2.32 +/- 1.16

Figure 1: Monthly variation of IASI mid-tropospheric CO_2 v9.1 (dashed line) for Metop-A (left) and Metop-B (right) from July 2007 to November 2020 and of CONTRAIL CO_2 (full line) from July 2007 to December 2016.

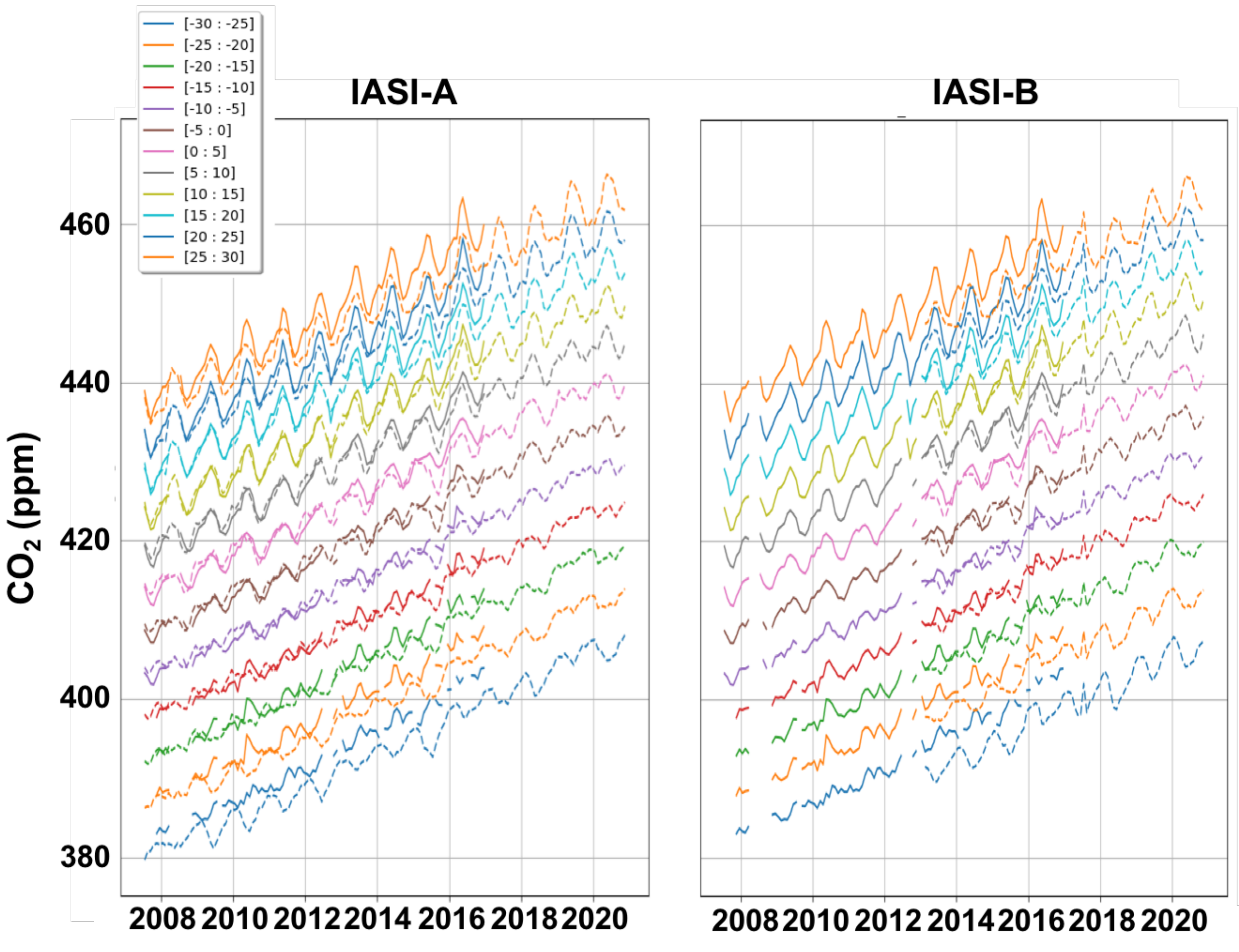

Figure 2: Scatter plot of IASI mid-tropospheric CO_2 v9.1 (IASI-A on left and IASI-B on right) vs. CONTRAIL CO_2 measured at 10 km over the whole period available for CONTRAIL depicted in Fig. 1 (July 2007 – December 2016) measured by aircraft at 10-12 km (dashed line) in 12 latitudinal bands of 5° each.

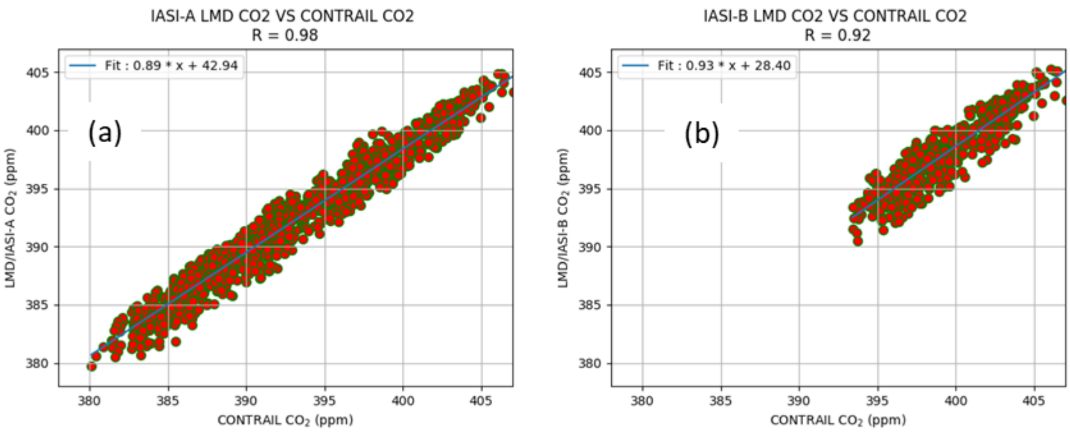

The relative systematic error is computed as the standard deviation of the CONTRAIL – IASI bias obtained in each latitudinal band. It is computed as two values:

- the "relative spatial bias", which is the standard deviation of the mean per-latitudinal band bias computed over the entire time series. It comes to 0.96 ppm.
- The "relative spatio-temporal bias", which is the standard deviation of the seasonal mean bias in each latitudinal band (i.e. JFM, AMJ, JAS, OND). It comes to 1.09 ppm.

For each latitudinal band, the linear drift was computed as the slope of the linear regression of the mean CONTRAIL –IASI bias against time. Table 3 shows the resulting drift and error. The main drift over the whole bands is: 0.06 ± 0.10 ppm/year.

Table 3: Linear drift of CO_2 (ppm).

Latitudinal band	30S: 25S	25S: 20S	20S: 15S	15S: 10S	10S: 5S	5S :EQ	EQ: 5N	5N: 10N	10N: 15N	15N: 20N	20N: 25N	25N: 30N
Linear drift [ppm/year]	0.01	-0.06	-0.02	-0.02	-0.02	-0.06	0.06	0.12	0.20	0.24	0.14	0.11

Finally, the year-to-year stability in each latitudinal band was computed as the difference between the maximum and the minimum values of the monthly differences within each year. This stability was found to be 2.78 ± 0.81 ppm/year.

2.1.1.2 Consistency between Metop-A and Metop-B

A direct comparison between mid-tropospheric CO_2 fields retrieved from Metop-A and Metop-B (version V9.1) yields a global bias and standard deviation of -0.28 ppm +/- 0.69 ppm.

Figure 3 shows the full time series of mid-tropospheric CO_2 retrieved from Metop-A and Metop-B. For most of the common period, the two products, which are recorded at the same local time but with a 180° shift in the orbit, are on top of each other. However, in 2020, the CO_2 retrieved from IASI/Metop-A is lower than the one retrieved from IASI/Metop-B. This is linked to a change in the correction of the detectors non linearity on Metop-A by the end of 2019. This change at instrument level has impacted the radiances themselves in the longwave band of IASI spectrum where the CO_2 absorption bands are located. The full characterization of this change is on-going. Once the impact has been properly characterized at Level 1, a correction of the radiances will be made and taken into account in the retrieval process.

Figure 3: Mid-tropospheric CO_2 retrieved from IASI/AMSU onboard Metop-A (blue) between July 2007 and November 2020, and from IASI/AMSU onboard Metop-B (blue) between February 2013 and November 2020.

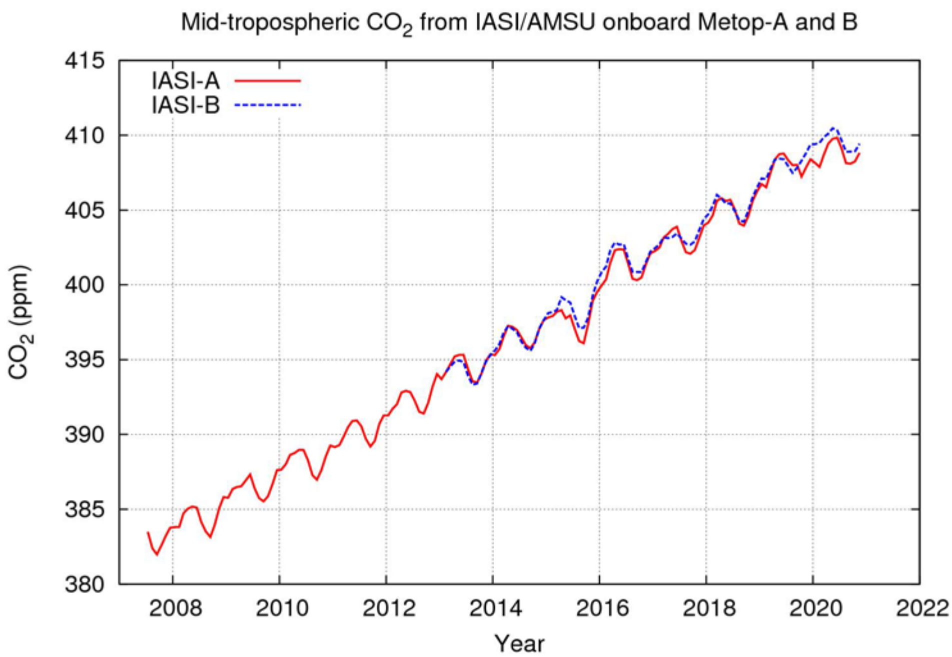

Figure 4 shows the seasonal maps (3 month average) of mid-tropospheric CO_2 retrieved from Metop-A and Metop-B, as well as the difference between the two and the associated standard deviation, over the whole period common between the instruments (2014-2020). The Metop-A and -B derived fields are close to each other. However, a small but positive bias for latitudes higher than 30 degrees can be seen. These biases appear to be constant throughout the year. Such constant biases might be due to the change from a tropical air mass to a mid-latitude air mass that is not consistent between the two instruments; this point will be checked for future releases.

Figure 4: Seasonal maps (3 month average) of mid-tropospheric CO_2 as retrieved from Metop-A (1st column), Metop-B (2nd column), and mean (3rd column) and standard deviation (4th column) of the difference between Metop-A and Metop-B , average over 2014-2020.

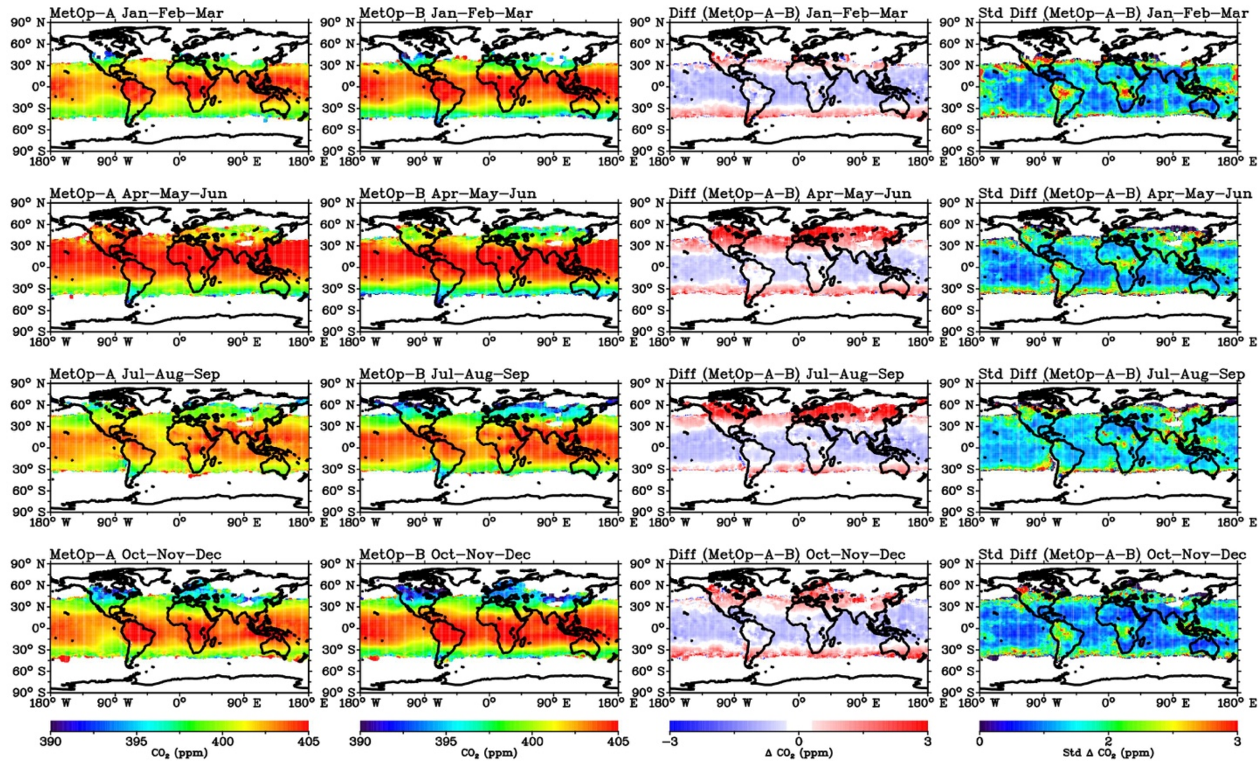

2.1.2 Validation summary

The validation results are summarized in the table below.

Table 4: Product Quality Summary Table for product CO2_IASA_NLIS.

Product Quality Summary Table for Product: CO2_IASA_NLIS Level: 2, Version: 9.1, Time period covered: 7.2007 – 11.2020				
Parameter [unit]	Achieved performance	Requirement	TR	Comments
Single measurement precision (1-sigma) in [ppm]	0.99	< 8 (T) < 3 (B) < 1 (G)	-	-
Mean bias [ppm]	0.96	-	-	No requirement but value close to zero expected for a high quality data product.
Accuracy: Relative systematic error [ppm]	Spatial – spatiotemporal: 0.96 / 1.09	< 0.5	Probability that accuracy TR is met: 50%	This value is based on the comparison between partial column and point measurement.
Stability: Drift [ppm/year]	0.06 ± 0.10 (1-sigma)	< 0.5	Probability that stability TR is met: 100%	-
Stability: Year-to-year bias variability [ppm/year]	2.78 ± 0.81 (1-sigma)	< 0.5	-	-

2.2 Products CH4_IASA_NLIS and CH4_IASB_NLIS

2.2.1 Validation

For CH_4 products, only two quantities have been evaluated so far: single measurement precision, and mean bias with both aircraft and AirCore measurements. Due to limited time series of both aircraft and balloons, it has not yet been possible to evaluate the stability criteria.

2.2.1.1 Validation with aircraft measurements

Retrievals are compared with measurements made in the framework of the CONTRAIL project (*Machida et al., 2007, 2008; Matsueda et al., 2008; Sawa et al., 2015*). All IASI retrievals falling in a 5°x5° grid cell centered on each CONTRAIL measurement are averaged. Figure 5 shows the scatter plot of each pair of CONTRAIL / IASI CH_4. Over the whole dataset, the difference between CONTRAIL and IASI CH_4 is -3.38 ± 15.59 ppb, with a correlation R factor of 0.81 for IASI-A and 0.76 for IASI-B.

Figure 5: CONTRAIL CH_4 vs. IASI CH_4 (Metop-A on left and Metop-B on right) for all CONTRAIL measurements over July 2007-December 2017. The 1x1 line is shown as black.

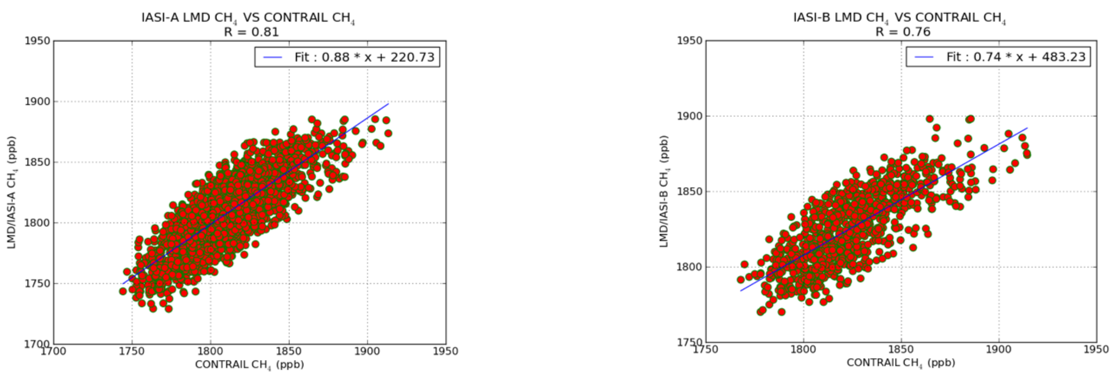

Figure 6 shows the monthly evolution of CH_4 as measured by CONTRAIL (dashed lines) and retrieved by IASI (full line) for 8 latitudinal bands of 10° each. The monthly evolution observed on both datasets is consistent whatever the latitude is, both in terms of seasonality and amplitude. Table 5 summarizes the statistics (mean and standard deviation) obtained within each 8 latitudinal bands for IASI, CONTRAIL and the difference between both. Both datasets are statistically in agreement. The standard deviations of IASI and CONTRAIL inside a given latitudinal band are noticeably close to each other.

Table 5: Mean and standard deviation of CH_4 (ppb): as measured by CONTRAIL aircrafts, as retrieved by IASI, and difference between the two over 7 latitudinal bands of 10° each. Statistics over July 2007-December 2017.

Latitudinal band	30S:40S	30S:20S	20S:10S	10S:EQ	EQ:10N	10N:20N	20N:30S	30N:40N
CONTRAIL	1807.98 ± 15.29	1795.43 ± 25.15	1792.49 ± 24.55	1810.47 ± 28.36	1827.10 ± 25.38	1830.52 ± 23.06	1835.80 ± 19.86	1807.98 ±15.29
IASI A	1812.81 ± 15.61	1798.55 ± 20.94	1800.85 ± 22.32	1812.30 ± 22.83	1824.71 ± 24.85	1831.64 ±24.12	1835.74 ±29.09	1812.81 ± 15.61
IASI-CONTRAIL	-4.83 ± 18.05	-3.12 ± 12.87	-8.37 ±11.68	-1.83 ± 15.40	2.38 ± 16.05	-1.11 ± 14.29	0.06 ± 20.08	-4.83 ± 18.05

Figure 6: Comparison between CONTRAIL and IASI CH_4 over July 2007-December 2017. Monthly evolution of CONTRAIL CH_4 (dashed line) and IASI CH_4 (full line) for 8 latitudinal bands of 10° each.

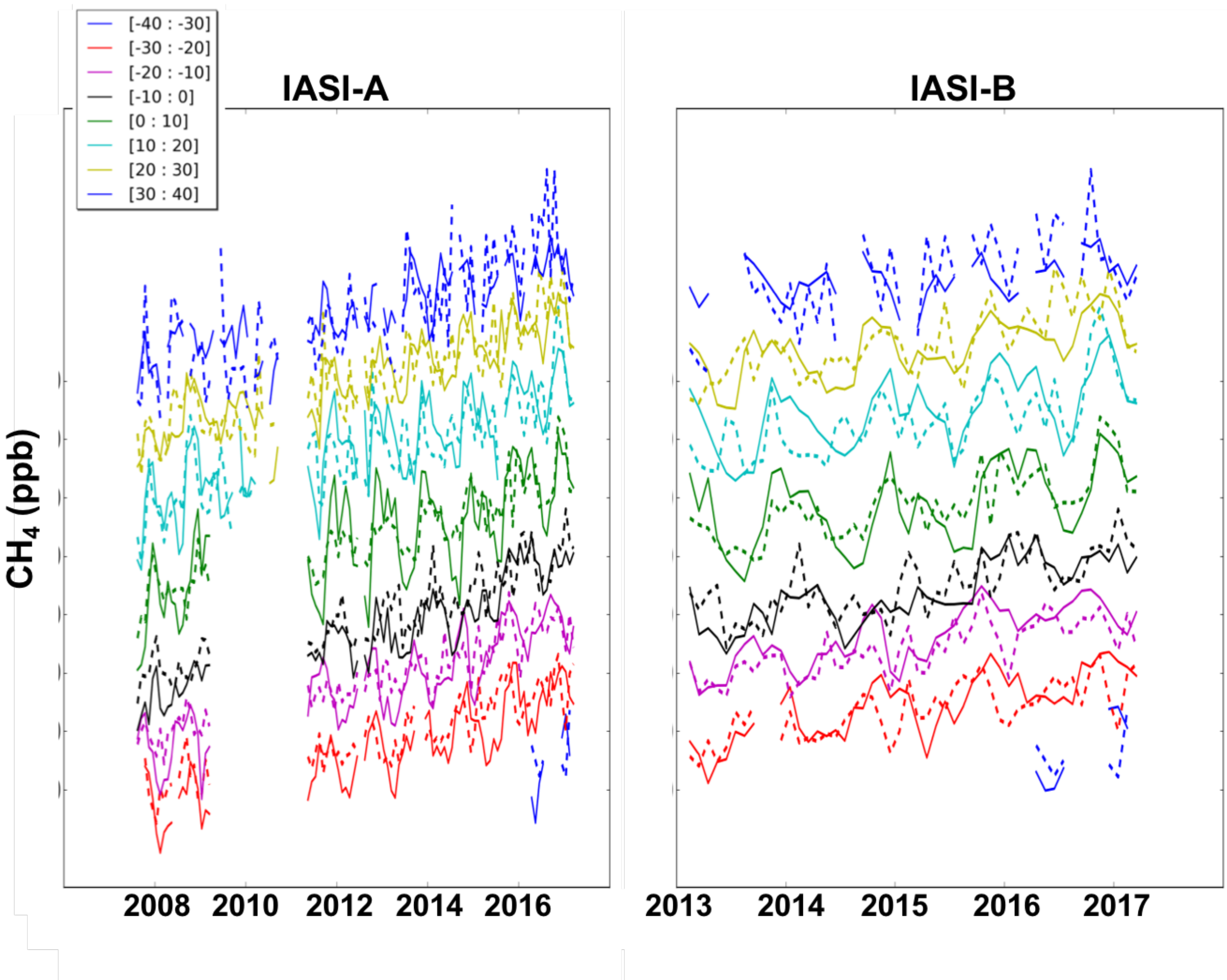

From Table 5, it is straightforward to compute the “relative spatial bias” of the “relative systematic error”, which is the standard deviation of the mean per-latitudinal band bias computed over the whole time series. The Accuracy is found to be 3.38 ppb. Due to several gaps in the time series, as well seen in Figure 6, it is not possible to compute the "relative spatio-temporal bias" which is the standard deviation of the seasonal mean bias in each latitudinal band.

2.2.1.2 Validation with AirCore 0-30 km profiles

Here, IASI CH_4 retrievals are compared to several AirCore profiles from measurements made by the French AirCore program (*Membrive et al., 2017, https://aircore.aeris-data.fr)*. All IASI retrievals falling in a 5°x5° grid cell centered on each AirCore profile for the same day are averaged. Figure 7 shows the scatter plot of each pair of AirCore/IASI CH_4. Over the whole dataset (44 pairs for Metop-A and for Metop-B), the difference between AirCore and IASI CH_4 is -1.97 ± 12.94 ppb.

Figure 7: Comparison between IASI CH_4 v9.1 and AirCore CH_4.

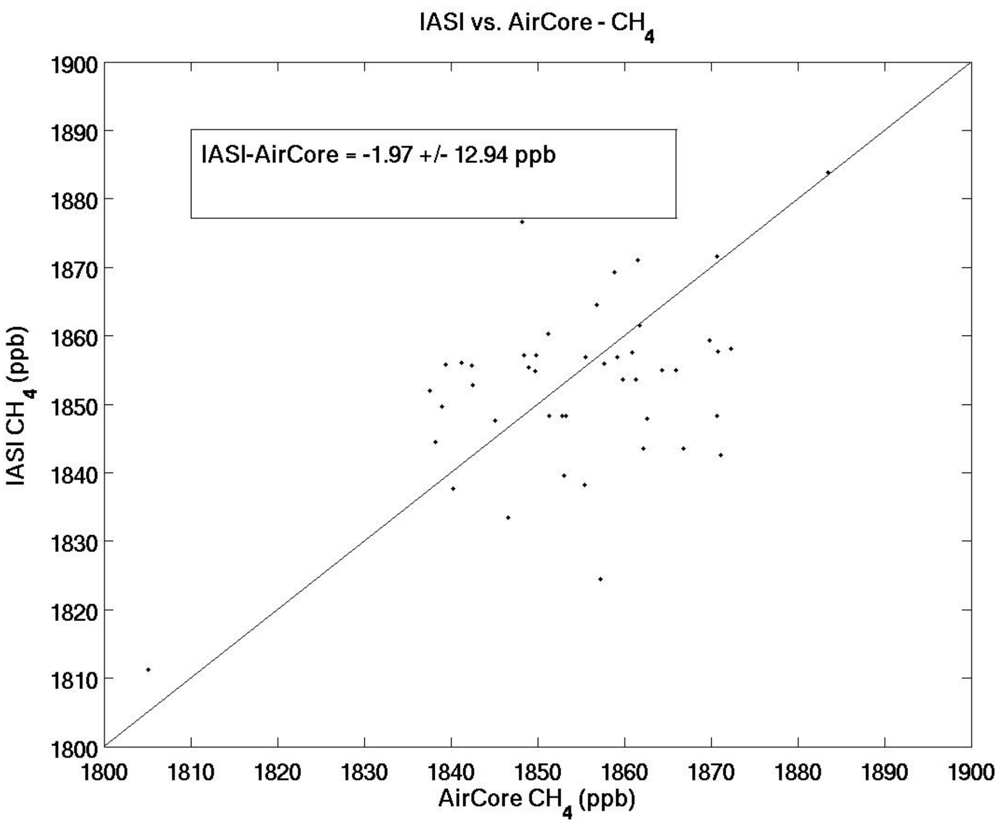

2.2.1.3 Comparison between CH4_IASA_NLIS (Metop-A) and CH4_IASB_NLIS (Metop-B)

A direct comparison between mid-tropospheric CH_4 fields retrieved from Metop-A and Metop-B (v9.1) yields a global difference of -3.43 ± 7.39 ppb. Figure 8 shows the seasonal maps (3 month average) of mid-tropospheric CH_4 retrieved from Metop-A and Metop-B, as well as the difference between the two and the associated standard deviation, over the time period 2014-2020. The Metop-A and -B derived fields are close to each other. However, a small but positive bias at latitude higher than 60 degrees can be observed on the map. These biases appear to be constant throughout the year.

Figure 8: Seasonal maps (3 month average) of mid-tropospheric CH_4 as retrieved from Metop-A (1st column), Metop-B (2nd column), and mean (3rd column) and standard deviation (4th column) of the difference between Metop-A and Metop-B, averaged over 2014-2020.

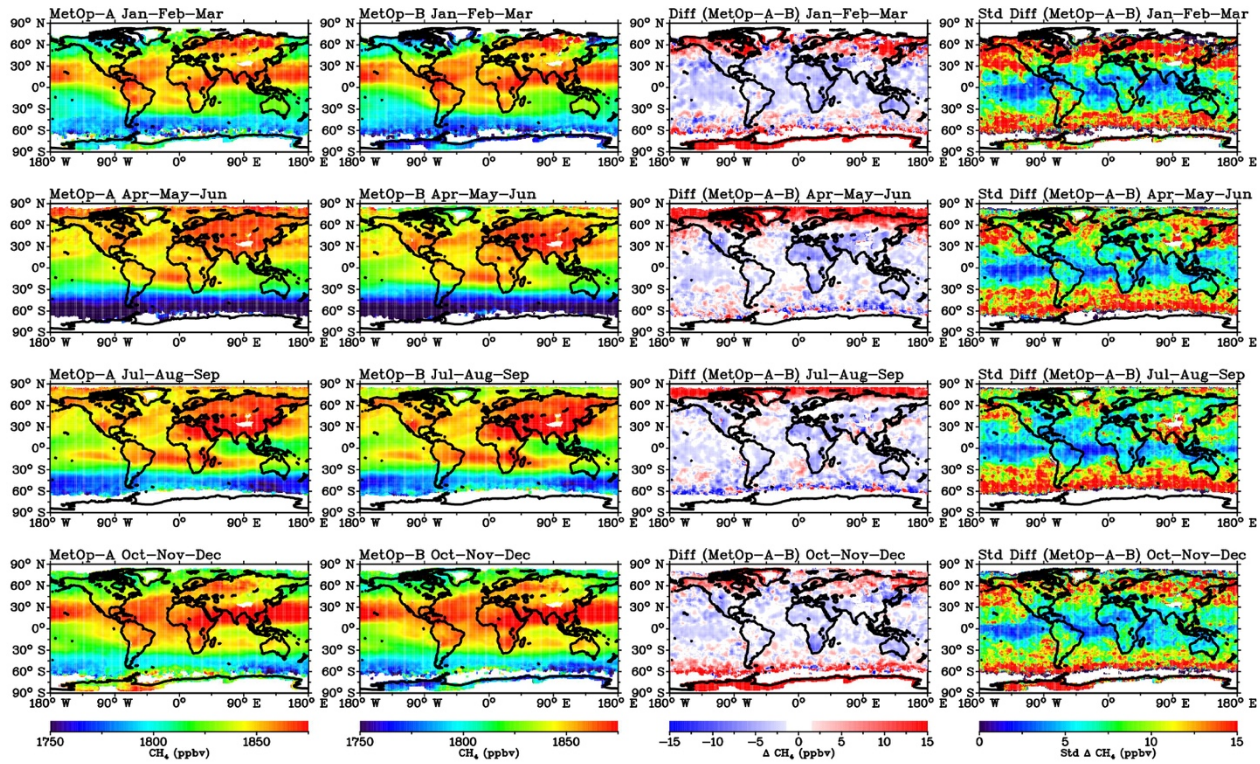

2.2.2 Validation summary

The validation results are summarized in the table below for CH4_IASA_NLIS. Please refer to Section 2.2.1.3 for comparison between CH4_IASA_NLIS and CH4_IASB_NLIS.

Table 6: Product Quality Summary Table for products CH4_IASA_NLIS (NC stands for Not computed due to lack of available data).

Product Quality Summary Table for Product: CH4_IASA_NLIS Level: 2, Version: 9.1, Time period covered: 7.2007 – 11.2020				
Parameter [unit]	Achieved performance	Requirement	TR	Comments
Single measurement precision (1-sigma) in [ppb]	11.8	< 34 (T) < 17 (B) < 9 (G)	-	-
Mean bias [ppb]	-3.38	-	-	No requirement but value close to zero expected for a high quality data product.
Accuracy: relative systematic error [ppb]	3.38	< 10	Probability that accuracy TR is met: 90%	-
Stability: Linear bias trend [ppb/year]	NC	< 3	NC	Time series of available aircraft/AirCore obs are not long enough to compute these 2 parameters
Stability: Year-to-year bias variability [ppb/year]	NC	< 3	-	

2.3 Product CO2_AIRS_NLIS

2.3.1 Validation

Use is made of in situ observations made by commercial airliners from April 1993 to March 2007 between Japan and Australia (data available at https://gaw.kishou.go.jp/). These observations, partly analyzed by *Matsueda et al. (2002)*, are available on a monthly basis. They cover the altitude range 9–13 km. Several gaps have affected the measurements throughout the period, which prevents making robust statistics from them.

The seasonal cycles of CO_2 measured by JAL are plotted in Fig. 9 for the period 2005-2006 (only period with full coverage). AIRS retrieved CO_2 cycle is also plotted in Fig. 9. There is a good agreement between both datasets in terms of the phase and amplitude of the seasonal cycle. Overall, the JAL – AIRS CO_2 difference is -0.43 ± 1.32 ppm.

Beginning of mid-2006, the bias between aircraft and AIRS CO_2 increases (negative sign), up to July 2007 when AIRS channels used to perform the retrievals were lost. This might be due to a non-corrected trend, which has affected either the AMSU observations in late 2006 and 2007, or some of the AIRS channels, which started exceeding radiometric specifications.

Figure 9: CO_2 seasonal cycle in the northern tropics as measured by JAL/CONTRAIL aircrafts (black) and as retrieved from AIRS (orange).

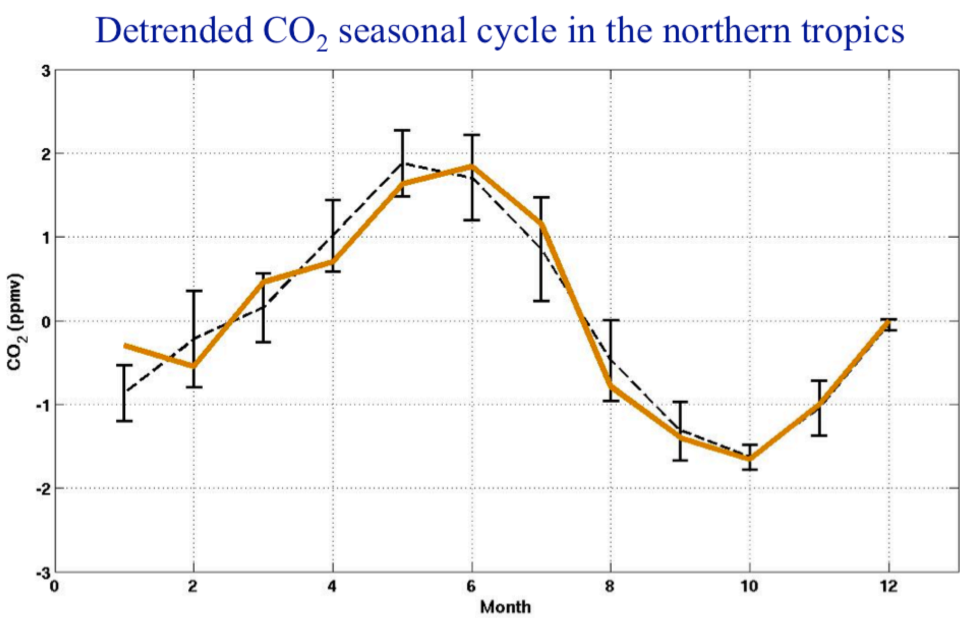

2.3.2 Validation summary

Table 7: Product Quality Summary Table for products CO2_AIRS_NLIS.

Product Quality Summary Table for Product: CO2_AIRS_NLIS Level: 2, Version: 3.0, Time period covered: 4.2003 – 7.2007				
Parameter [unit]	Achieved performance	Requirement	TR	Comments
Single measurement precision (1-sigma) in [ppb]	1.32	< 8 (T) < 3 (B) < 1 (G)	-	-
Mean bias [ppb]	-0.43	-	-	No requirement but value close to zero expected for a high quality data product.

References

Buchwitz et al., 2017: ESA Climate Change Initiative (CCI) Product Validation and Intercomparison Report (PVIR) for the Essential Climate Variable (ECV) Greenhouse Gases (GHG) for data set Climate Research Data Package No. 4 (CRDP#4), Version 5.0, 9. Feb. 2017, 2017.

Chédin et al. 2003: Chédin, A., Saunders, R., Hollingsworth, A., Scott, N. A., Matricardi, M., Etcheto, J., Clerbaux, C., Armante, R. and Crevoisier, C.: The feasibility of monitoring CO_2 from high resolution infrared sounders. J. Geophys. Res., 108, ACH 6-1–6-19, doi: 10.1029/2001JD001443, 2003.

Chevallier et al., 2005: Chevallier, F., R. J. Engelen, and P. Peylin, The contribution of AIRS data to the estimation of CO_2 sources and sinks. Geophys. Res. Lett., 32, L23801, doi:10.1029/ 2005GL024229, 2005.

CMUG-RBD, 2010: Climate Modelling User Group Requirements Baseline Document, Deliverable 1.2, Number D1.2, Version 1.3, 2 Nov 2010.

Cressot et al., 2014: Cressot, C., F. Chevallier, P. Bousquet, et al., On the consistency between global and regional methane emissions inferred from SCIAMACHY, TANSO-FTS, IASI and surface measurements, Atmos. Chem. Phys., 14, 577-592, 2014.

Crevoisier et al., 2004: Crevoisier, C., S. Heilliette, A. Chédin, S. Serrar, R. Armante, and N. A. Scott, Midtropospheric CO_2 concentration retrieval from AIRS observations in the tropics, Geophys. Res. Lett., 31, L17106, doi:10.1029/2004GL020141, 2004.

Crevoisier et al., 2009: Crevoisier, C., Chédin, A., Matsueda, H., et al., First year of upper tropospheric integrated content of CO_2 from IASI hyperspectral infrared observations, *Atmos. Chem. Phys.*, 9, 4797-4810, 2009.

Crevoisier et al. 2009b: Crevoisier, C., Nobileau, D., Fiore, A., Armante, R., Chédin, A., and Scott, N. A.: Tropospheric methane in the tropics – first year from IASI hyperspectral infrared observations, Atmos. Chem. Phys., 9, 6337–6350, doi:10.5194/acp-9-6337-2009, 2009b.

Crevoisier et al., 2013: Crevoisier, C., Nobileau, D., Armante, R., et al., The 2007–2011 evolution of tropical methane in the mid-troposphere as seen from space by MetOp-A/IASI, *Atmos. Chem. Phys.*, 13, 4279-4289, 2013.

GCOS-154: Global Climate Observing System (GCOS): SYSTEMATIC OBSERVATION REQUIREMENTS FOR SATELLITE-BASED DATA PRODUCTS FOR CLIMATE - 2011 Update - Supplemental details to the satellite-based component of the "Implementation Plan for the Global Observing System for Climate in Support of the UNFCCC (2010 Update)", December 2011, prepared by World Meteorological Organization (WMO), Intergovernmental Oceanographic Commission, United Nations Environment Programme (UNEP), International Council for Science, Doc.: GCOS 154, 2011.

GCOS-200: The Global Observing System for Climate: Implementation Needs, World Meteorological Organization (WMO), GCOS-200 (GOOS-214), pp. 325, link: http://unfccc.int/files/science/workstreams/systematic_observation/application/pdf/gcos_ip_10oct2016.pdf, 2016.

Jacquinet-Husson et al. 2011: Jacquinet-Husson N., L. Crépeau, R. Armante, C. Boutammine, A. Chédin, et al.. The 2009 edition of the GEISA spectroscopic database, J. Quant. Spectrosc. Radiat. Transfer,112, 2395-2445 doi:10.1016/j.jqsrt.2011.06.004, 2011.

Machida et al. 2008: Machida, T., Matsueda, H., Sawa, Y., Nakagawa, Y., Hirotani, K., Kondo, N., Goto, K., Nakazawa, T., Ishikawa, K., and Ogawa, T.: Worldwide measurements of atmospheric CO_2 and other trace gas species using commercial airlines, J. Atmos. Ocean. Tech., 25(10), 1744–1754, doi:10.1175/2008JTECHA1082.1, 2008.

Matsueda et al. 2008: Matsueda, H., Machida, T., Sawa, Y., Nakagawa, Y., Hirotani, K., Ikeda, H., Kondo, N., and Goto, K.: Evaluation of atmospheric CO_2 measurements from new flask air sampling of JAL airliner observation, Pap. Meteorol. Geophys., 59, 1–17, 2008.

Membrive et al. 2017: Membrive, O., Crevoisier, C., Sweeney, C., Danis, F., Hertzog, A., Engel, A., Bönisch, H., and Picon, L.: AirCore-HR: a high-resolution column sampling to enhance the vertical description of CH_4 and CO_2, Atmos. Meas. Tech., 10, 2163-2181, https://doi.org/10.5194/amt-10-2163-2017, 2017.

Sawa et al. 2015: Sawa, Y., Machida, T., Matsueda, H., Niwa, Y., Tsuboi, K., Murayama, S., Morimoto, S., and Aoki, S.: Seasonal changes of CO_2, CH_4, N_2O, and SF_6 in the upper troposphere/lower stratosphere over the Eurasian continent observed by commercial airliner, Geophys. Res. Lett., 42, 2001–2008, https://doi.org/10.1002/2014GL062734, 2015.

Scott and Chédin 1981: Scott N.A. and Chédin A., A fast line-by-line method for atmospheric absorption computations: The Automatized Atmospheric Absorption Atlas, J. Appl. Meteor., 20, n° 7, pp. 802-812, 1981.

TRD GHG, 2017: Buchwitz, M., Aben, I., Anand, J., Armante, R., Boesch, H., Crevoisier, C., Detmers, R. G., Hasekamp, O. P., Reuter, M., Schneising-Weigel, O., Target Requirement Document, Copernicus Climate Change Service (C3S) project on satellite-derived Essential Climate Variable (ECV) Greenhouse Gases (CO_2 and CH_4) data products (project C3S_312a_Lot6), Version 1, 28-March-2017, pp. 52, 2017.

TRD GAD GHG, 2020: Buchwitz, M., Aben, I., Armante, R., Boesch, H., Crevoisier, C., Hasekamp, O. P., Wu, L.., Reuter, M., Schneising-Weigel, O., Target Requirement and Gap Analysis Document, Copernicus Climate Change Service (C3S) project on satellite-derived Essential Climate Variable (ECV) Greenhouse Gases (CO_2 and CH_4) data products (project C3S_312b_Lot2), Version 2.11, 9-April-2020, pp. 80, 2020.

Wofsy et al. 2012: Wofsy, S. C., Daube, B. C., Jimenez, R., et al.: HIPPO Merged 10-second Meteorology, Atmospheric Chemistry, Aerosol Data (R 20121129), Carbon Dioxide Information Analysis Center, Oak Ridge National Laboratory, Oak Ridge, Tennessee, USA, http://dx.doi.org/, 10.3334/CDIAC/hippo 010 (Release 29 November 2012), 2012.

Yoshida et al. 2013: Yoshida, Y., Kikuchi, N., Morino, I., Uchino, O., Oshchepkov, S., Bril, A., Saeki, T., Schutgens, N., Toon, G. C., Wunch, D., Roehl, C. M., Wennberg, P. O., Griffith, D. W. T, Deutscher, N. M., Warneke, T., Notholt, J., Robinson, J., Sherlock, V., Connor, B., Rettinger, M., Sussmann, R., Ahonen, P., Heikkinen, P., Kyrö, E., Mendonca, J., Strong, K., Hase, F., Dohe, S., and Yokota, T.: Improvement of the retrieval algorithm for GOSAT SWIR XCO_2 and XCH_4 and their validation using TCCON data, Atmos. Meas. Tech., 6, 1533–1547, doi:10.5194/amt-6-1533-2013, 2013.

Copernicus Climate Change Service

ECMWF - Shinfield Park, Reading RG2 9AX, UK

Contact: info@copernicus-climate.eu